Second Law Approach for Turbulent Flow in an Annular Duct Partly Filled with a Porous Substrate

N. Allouache, S. Chikh

Abstract—The paper is aimed at investigating the turbulent flow and heat transfer characteristics in an annular duct partly filled with a porous medium. A modified $k-\varepsilon$ model for approximating the Forchheimer term in the equations of turbulent kinetic energy and dissipation rate is developed by time-averaging the general macroscopic transport equations. This model accounts for the second order approximation in the Forchheimer term. This higher order term leads to a better description of the turbulent effects of the Forchheimer term in the flow through the porous medium. A second law approach, based on the entropy generation is used, in order to find the compromise between hydrodynamics and thermal performances.

Index Terms—Heat transfer, second law analysis, porous medium, turbulent flow, numerical modeling.

I. Introduction

There has been a great interest lately regarding turbulent flow in porous media. This is related to their potential industrial applications such as packed bed reactors, filtering insulation, grain storage and drying, electronic cooling and heat exchangers. Two different approaches for developing macroscopic models for incompressible flow in saturated porous media were found in the literature. In the first approach, the governing equations are obtained by time averaging the volume-averaged equations [1,2]. In the second approach, a volume average operator is applied to the local time-averaged equations [3]. Silva and de Lemos [4] discussed different aspects of macroscopic modeling of turbulence in homogeneous porous media. All these approaches rely on a two-equation macroscopic turbulence model ($k-\varepsilon$). Using the first approach, a modified model is developed to analyze turbulent flow in a duct partly filled with a porous matrix.

Improving heat exchanger effectiveness by enhancement techniques is always achieved at the expense of fluid friction losses; an optimal trade-off has become the critical challenge for the design work. The optimal design can be achieved if the second law of thermodynamics is accounted for. The study of second law in turbulent flow with a porous media is almost no existent. The majority of studies are presented for laminar flows [5-7]. A model equation for calculation of the local entropy generation in the turbulent shear flow is used.

The hot fluid flows in the inner cylinder and the cold one in the annular gap. The porous substrate is attached to the inner cylinder and the outer cylinder is perfectly insulated. The investigation is performed taking into account the effects of various parameters such as the Reynolds number, the porous layer thickness, the permeability and the effective thermal conductivity.

II. Numerical Modeling

The fluid is assumed to be incompressible and the flow two-dimensional and axisymmetric. The porous substrate is considered homogeneous, isotropic and saturated with a single-phase. The fluid is in local thermal equilibrium with the solid matrix.

A. Governing Equations

The final average continuity, momentum, and energy, in cylindrical coordinates are [8]:

Continuity equation:

$$\frac{\partial U}{\partial z} + \frac{1}{r}\frac{\partial (rV)}{\partial r} = 0 \tag{1}$$

Momentum equation in axial direction

$$U\frac{\partial U}{\partial z} + \frac{V}{r}\frac{\partial (rU)}{\partial r} = -\frac{1}{\rho_f}\frac{\partial P}{\partial z} + \frac{\partial}{\partial z}\left((\nu_t + \nu J)\frac{\partial U}{\partial z}\right)$$
$$+ \frac{1}{r}\frac{\partial}{\partial r}\left((\nu_t + \nu J)r\frac{\partial U}{\partial r}\right) - \frac{2}{3}\frac{\partial k}{\partial z} + \frac{\partial}{\partial z}\left(\nu_t\frac{\partial U}{\partial z}\right)$$
$$+ \frac{1}{r}\frac{\partial}{\partial r}\left(\nu_t r\frac{\partial V}{\partial z}\right) - \phi\frac{\nu}{K}U - \phi^2\frac{c_F}{K^{1/2}}$$
$$\left(|U|U + \frac{1}{|U|}\left(\frac{2}{3}kU - \nu_t\left(2U\frac{\partial U}{\partial z} + V\left(\frac{\partial U}{\partial r} + \frac{\partial V}{\partial z}\right)\right)\right)\right) \tag{2}$$

Momentum equation in radial direction:

$$U\frac{\partial V}{\partial z}+\frac{V}{r}\frac{\partial (rV)}{\partial r}=-\frac{1}{\rho_f}\frac{\partial P}{\partial z}+\frac{\partial}{\partial z}\left((v_t+vJ)\frac{\partial V}{\partial z}\right)$$
$$+\frac{1}{r}\frac{\partial}{\partial r}\left((v_t+vJ)r\frac{\partial V}{\partial r}\right)-\frac{2}{3}\frac{\partial k}{\partial z}+\frac{\partial}{\partial z}\left(v_t\frac{\partial V}{\partial r}\right)$$
$$+\frac{1}{r}\frac{\partial}{\partial r}\left(v_t r\frac{\partial V}{\partial r}\right)-\frac{2v_t V}{r^2}-\phi\frac{v}{K}V-\phi^2\frac{c_F}{K^{1/2}}$$
$$\left(|U|V+\frac{1}{|U|}\left(\frac{2}{3}kV-v_t\left(2V\frac{\partial V}{\partial r}+V\left(\frac{\partial V}{\partial z}+\frac{\partial U}{\partial r}\right)\right)\right)\right)$$

(3)

U,V are the time-averaged fluid velocities, $v_t=C_\mu k^2/\varepsilon$ is the eddy viscosity, ϕ is the porosity, K is the porous medium permeability and $J=\mu_e/\mu_f$ is the viscosity ratio .

Model equation for turbulent kinetic energy (k):

$$U\frac{\partial k}{\partial z}+\frac{V}{r}\frac{\partial (rk)}{\partial r}=P_k+\frac{\partial}{\partial z}\left(\left(vJ+\frac{v_t}{\sigma_k}\right)\frac{\partial k}{\partial z}\right)$$
$$+\frac{1}{r}\frac{\partial}{\partial r}\left(\left(vJ+\frac{v_t}{\sigma_k}\right)r\frac{\partial k}{\partial r}\right)-J\varepsilon-G_k$$

(4)

where

$$P_k=v_t\left(2\left(\frac{\partial V}{\partial r}\right)^2+2\left(\frac{\partial U}{\partial z}\right)^2+\left(\frac{\partial V}{\partial z}+\frac{\partial U}{\partial r}\right)^2+2\left(\frac{V}{r}\right)^2\right)$$

(5)

$$G_k=2\phi\frac{v}{K}k+\frac{\phi^2 c_F}{K^{1/2}|U|}\left(-\frac{4}{3}C_s\frac{k^2}{\varepsilon}\left(\frac{5}{3}\left(U\frac{\partial k}{\partial z}+V\frac{\partial k}{\partial r}\right)\right.\right.$$
$$-\left(2U\frac{\partial}{\partial z}\left(v_t\frac{\partial U}{\partial z}\right)+2\frac{V}{r}\frac{\partial}{\partial r}\left(v_t r\frac{\partial V}{\partial r}\right)-\frac{2v_t V}{r^2}\right.$$
$$+V\frac{\partial}{\partial z}v_t\left(\frac{\partial U}{\partial r}+\frac{\partial V}{\partial z}\right)+\frac{U}{r}\frac{\partial}{\partial r}v_t r\left(\frac{\partial V}{\partial z}+\frac{\partial U}{\partial r}\right)\right)$$
$$\left.\left.+\frac{8}{3}(U^2+V^2)k-\frac{2v_t}{|U|}\left(U^2\frac{\partial U}{\partial z}+V^2\frac{\partial V}{\partial r}+UV\left(\frac{\partial U}{\partial r}+\frac{\partial V}{\partial z}\right)\right)\right)\right)$$

(6)

Model equation for dissipation rate (ε):

$$U\frac{\partial\varepsilon}{\partial z}+\frac{V}{r}\frac{\partial(r\varepsilon)}{\partial r}=\frac{\partial}{\partial z}\left(\left(vJ+\frac{v_t}{\sigma_\varepsilon}\right)\frac{\partial\varepsilon}{\partial z}\right)+\frac{1}{r}\frac{\partial}{\partial r}\left(\left(vJ+\frac{v_t}{\sigma_\varepsilon}\right)\frac{\partial\varepsilon}{\partial r}\right)$$
$$+C_{\varepsilon1}\frac{\varepsilon}{k}P_k-C_{\varepsilon2}\frac{\varepsilon^2}{k}-2\phi\frac{v}{K}\varepsilon-2\phi^2\frac{c_F}{K^{1/2}}\left(\frac{4}{3}|U|\varepsilon+\frac{1}{|U|}\left(C_{\varepsilon3}\frac{k}{\varepsilon}\right.\right.$$
$$\left(\left(2v_t U\frac{\partial U}{\partial z}-\frac{2}{3}kU\right)\frac{\partial\varepsilon}{\partial z}+\left(2v_t V\frac{\partial V}{\partial r}-\frac{2}{3}kV\right)\frac{\partial\varepsilon}{\partial r}+Uv_t\left(\frac{\partial U}{\partial r}+\frac{\partial V}{\partial z}\right)\frac{\partial\varepsilon}{\partial r}\right.$$
$$\left.+Vv_t\left(\frac{\partial V}{\partial z}+\frac{\partial U}{\partial r}\right)\frac{\partial\varepsilon}{\partial z}\right)+\frac{4}{3}v\frac{\partial|U|}{\partial z}\frac{\partial k}{\partial z}+\frac{4}{3}v\frac{\partial|U|}{\partial r}\frac{\partial k}{\partial r}$$
$$-v\left(\frac{\partial}{\partial z}\left(\frac{U^2}{|U|}\right)\frac{\partial}{\partial z}\left(v_t\frac{\partial U}{\partial z}\right)+\frac{\partial}{\partial r}\left(\frac{U^2}{|U|}\right)\frac{\partial}{\partial r}\left(\frac{\partial U}{\partial z}\right)\right)$$
$$+\frac{\partial}{\partial z}\left(\frac{UV}{|U|}\right)\frac{\partial}{\partial z}\left(v_t\left(\frac{\partial U}{\partial r}+\frac{\partial V}{\partial z}\right)\right)+\frac{\partial}{\partial r}\left(\frac{UV}{|U|}\right)\frac{\partial}{\partial r}\left(v_t\left(\frac{\partial U}{\partial r}+\frac{\partial V}{\partial z}\right)\right)$$
$$\left.\left.+\frac{\partial}{\partial z}\left(\frac{V^2}{|U|}\right)\frac{\partial}{\partial z}\left(v_t\frac{\partial V}{\partial r}\right)+\frac{\partial}{\partial r}\left(\frac{V^2}{|U|}\right)\frac{\partial}{\partial r}\left(v_t\frac{\partial V}{\partial r}\right)\right)\right)$$

(7)

Energy equation:

$$U\frac{\partial\overline{T}}{\partial z}+\frac{V}{r}\frac{\partial (r\,\overline{T})}{\partial r}=\frac{\partial}{\partial z}\left(\left(\frac{R_c\,v}{\phi\,\mathrm{Pr}}+\frac{v_t}{\sigma_t}\right)\frac{\partial\overline{T}}{\partial z}\right)$$
$$+\frac{1}{r}\frac{\partial}{\partial r}\left(\left(\frac{R_c\,v}{\phi\,\mathrm{Pr}}+\frac{v_t}{\sigma_t}\right)r\frac{\partial\overline{T}}{\partial r}\right)$$

(8)

$\overline{T}$ is the average temperature, Pr is the Prandtl number and $R_c=\lambda_e/\lambda_f$ is the thermal conductivity ratio.

C_μ, $C_{\varepsilon1}$, $C_{\varepsilon2}$, $C_{\varepsilon3}$, C_s, σ_κ, σ_ε and σ_t are the constants used in the transport equations [8].

u′,v′,T′ are fluctuating quantities. The subscript j in λ_j and μ_j stands for h in the hot side and for c in the cold side. While in the porous region, j indicates the effective thermal conductivity in k_j. Eq. (8) can be written as:

$$\dot{S}_g=\dot{S}_{\Delta\overline{T}}+\dot{S}_{\Delta T'}+\dot{S}_{\Delta p}+\dot{S}_{\Delta p'}$$

(9)

In Eq. (9), the first and second groups of terms describe the heat transfer entropy production due respectively to time mean temperature gradients and fluctuating temperature gradients. The third and fourth groups of terms containing respectively the mean and fluctuating velocity gradients represent the entropy production due to fluid friction. The model equations for the fluctuating quantities $\dot{S}_{\Delta T'}$ and $\dot{S}_{\Delta p'}$ are [9]:

$$\dot{S}_{\Delta T'}=C_p\,\mu_t/\sigma_t\,\lambda_j\,\dot{S}_{\Delta\overline{T}}$$

(10)

$$\dot{S}_{\Delta p'}=\rho\,\varepsilon/\overline{T}$$

(11)

The rate of entropy generation over the cross section is calculated by integration:

$$S_g=\int_0^{r_i}\dot{S}_g\,2\pi r\,dr$$

(12)

The irreversibility distribution ratio (Ψ) is defined as:

$$\Psi=S_{\Delta p}/S_{\Delta T}$$

(13)

B. Boundary conditions

The associated conditions are:
- Prescribed velocities, temperatures, turbulent kinetic energies and dissipation rates at the inlet.
- Velocity and turbulent kinetic energy are set equal to zero, and $\varepsilon=v\,\partial^2 k/\partial r^2$, at the walls.
- The outer cylinder is perfectly insulated.
- A wall function approach was used for treating the flow close to the wall [8].
- At the porous-clear fluid interface, the stress jump is described by an adjustable coefficient β which accounts for the stress jump at the interface, as in [4]:

$$(\mu + \mu_t)\frac{\partial U}{\partial r}\bigg|_f - (\mu_e + \mu_t)\frac{\partial U}{\partial r}\bigg|_p = (\mu + \mu_t)\frac{\beta}{\sqrt{K}}U\bigg|_{interface} \quad (14)$$

$$\left(\mu + \frac{\mu_t}{\sigma_k}\right)\frac{\partial k}{\partial r}\bigg|_f - (\mu_e + \frac{\mu_t}{\sigma_k})\frac{\partial k}{\partial r}\bigg|_p = (\mu + \mu_t)\frac{\beta}{\sqrt{K}}k\bigg|_{interface} \quad (15)$$

A. Numerical Procedure

The Numerical method employed for discretizing the governing equations is the control-volume approach. The well-established SIMPLE algorithm is followed for handling the pressure-velocity coupling. The set of the discretized linear algebraic equations with associated boundary conditions is solved using the line by line procedure. The convergence is monitored in terms of the normalized residue of the algebraic equation. The maximum residue allowed for convergence check is set to 10^{-4}.

III. RESULTS

The results are presented for water flow in an annular duct of diameter ratio equal to 2. The effective viscosity in the porous medium equals the fluid viscosity (Brinkman assumption, J=1). The porosity of the porous material equals 0.95 and the inertia coefficient in the porous medium C_F is taken equal to 0.1.

On the basis that a flow is turbulent in a porous domain if pore Reynolds number is over 300, the limiting curve is located for each value of Darcy number characterizing the permeability of the porous material ($D = K/D_h^2$). The results show an existence of two different zones, in the annular space, as function of the hydraulic Reynolds number and the permeability (Fig. 1), the zone where the flow is fully turbulent in both clear fluid and porous regions and the zone where the flow is relaminarized in the porous region.
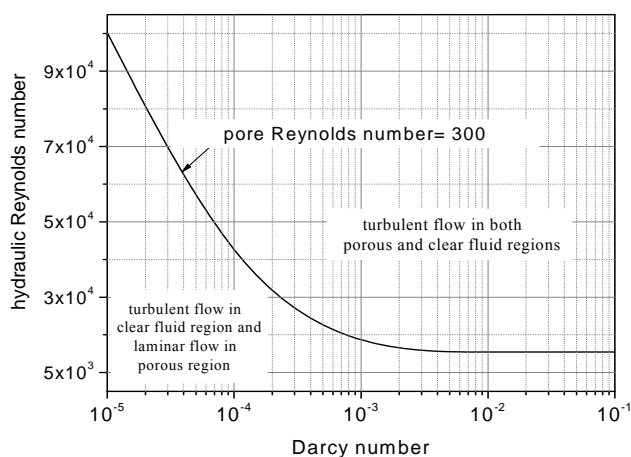

Fig. 1. Hydraulic Reynolds number vs Darcy number.

The following results are presented for the considered hydraulic Reynolds number ($Re_H = \mu_{in}D_h/v_f$) $Re_H = 5.2\times10^4$.

Fig. 2 displays the axial velocity profile in the radial direction when the porous layer occupies 40% of the annular space. The porous matrix forces the fluid to escape to the clear region. This is due to the additional delay of the

flow caused by the microscopic inertial and viscous forces caused by the porous matrix. For small Darcy numbers, the porous material presents a high resistance to the flow.
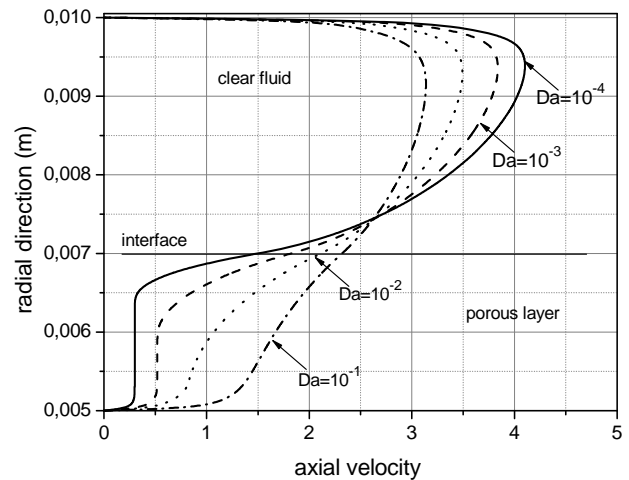

Fig. 2. Axial velocity profiles for different Darcy number.

An increase in the effective thermal conductivity (R_c) of the porous medium improves considerably the temperature of the cold fluid at the exit of the duct (Fig. 3). Furthermore, there exists a critical value of the porous layer thickness bellow which the cold fluid temperature is increased and thus the heat transfer is improved and even passes the one of the fluid case without the porous substrate (fluid case).
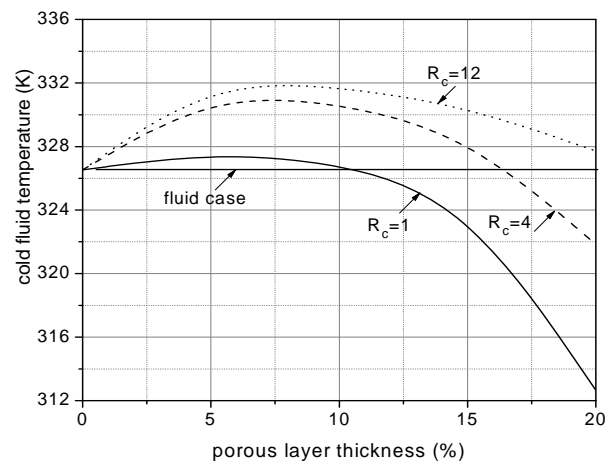

Fig. 3. Cold fluid temperature vs porous layer thickness.

The evolution of the total entropy generation rate due to both fluid friction and heat transfer in the annular space for different values of inlet temperature difference between the hot and cold fluids (ΔT_{in}) is presented in Fig. 4. As it is seen, an increase in the inlet temperature difference leads to an increase in the in the rate of total entropy generation. For high values of inlet temperature difference ($\Delta T_{in} > 20°C$), there exist optimal and critical porous layer thicknesses of which two minima and maximum entropy generation rate due to heat transfer are obtained, for each value of Darcy number. The first minimum located before the maximum is

lower than the one located after the maximum. A highly permeable porous substrate yields smaller values of first minimum and maximum entropy generation rate, and a higher value of second minimum entropy generation rate.
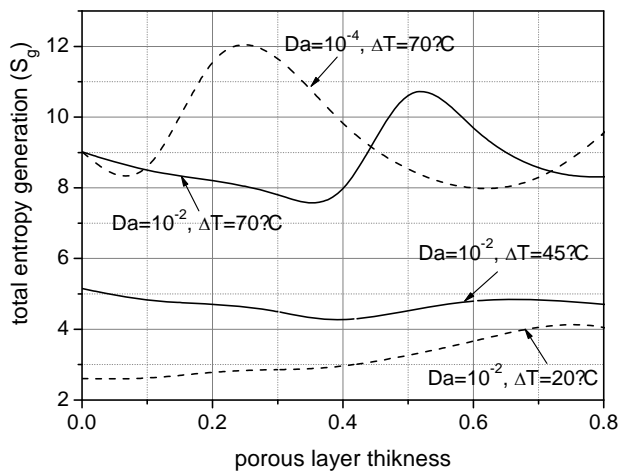

Fig. 4. Effect of porous layer thickness, Darcy number and ΔT_{in} on total entropy generation.

The evolution of the irreversibility distribution ratio, which is defined as the ratio of the fluid friction irreversibility to heat transfer irreversibility, is shown in fig. 5. clearly, the irreversibility distribution ratio is less important for high values of ΔT_{in} ($\Delta T_{in} > 20°C$) and Darcy number. This means that the lost available work is mainly due to heat transfer as the entropy production due heat transfer is the prevailing contribution. on the other hand, for $\Delta T_{in} \leq 20°C$, the irreversibility due to fluid friction dominates. Also, we can notice that the irreversibility distribution ratio is more important for high values of porous layer thickness.
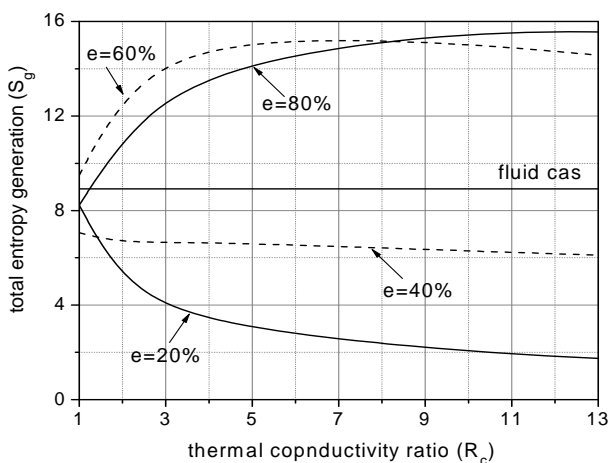

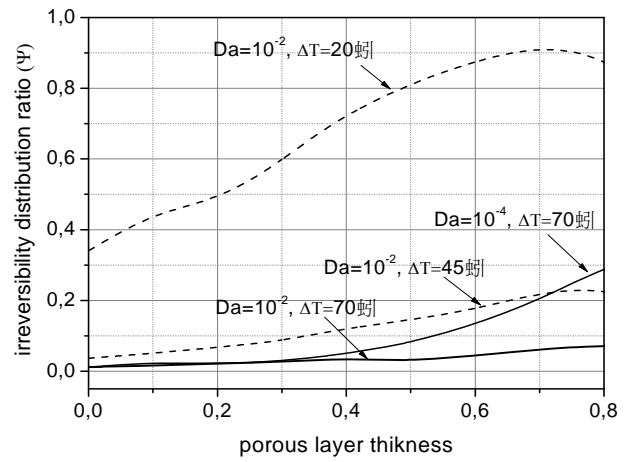Fig. 5. Effect of thermal conductivity and porous layer thickness on total entropy generation.

Fig. 6. Irreversibility distribution ration for different porous layer thickness, Darcy number and ΔT_{in}.

IV. NOMENCLATURE

TABLE I

Symbol	Quantity	Units
C_p	specific heat of fluid	J/(kg.K)
c_F	Forchheimer inertia coefficient	-
D_h	hydraulic diameter	m
Da	Darcy number	-
e	porous layer thickness	m
J	viscosity ratio	-
k	turbulent kinetic energy	m^2/s^2
K	Permeability	m^2
P	pressure	Pa
Pr	Prandtl number	-
r	radial direction	-
Re_H	hydraulic Reynolds number	-
R_c	conductivity ratio	-
$\dot{S}$	entropy generation rate per volume unit	$W/(m^3.K)$
S	entropy generation rate	W/K
$\overline{T}$	time averaged temperature	K
T'	fluctuation fluid temperature	K
u', v'	fluctuation fluid velocities	m/s
U	axial time-averaged fluid velocity	m/s
V	radial time-averaged fluid velocity	m/s
z	axial direction	-
λ	thermal conductivity	$W/(m^2.K)$
ρ	density	kg/m^3
μ	dynamic viscosity	kg/(m.s)
ν	kinematic viscosity	m^2/s
ε	dissipation rate	-
ϕ	Porosity	-
Subscript		
c	cold	
e	effective	
f	fluid	
h	hot	
in	inlet	
g	total	
p	porous	
t	turbulent	
ΔT	due to heat transfert	
ΔP	due to fluid friction	

Fig. 6 displays the effect of the thermal conductivity ratio on the total entropy generation. As it is seen, an increase in the thermal conductivity ratio leads to a considerable reduction of the total entropy production, for lower values of the porous layer thickness (e≤40%).

V. CONCLUSION

A modified $k-\varepsilon$ model that account for the higher Forchheimer term order is used to well simulate the turbulent flow in the porous annular duct. A second approach analysis is used to find the best conditions in order to minimize the entropy generation. The results show that the turbulent heat transfer and the entropy generation are noticeably influenced by the permeability, the layer thickness, the inlet difference temperature and the effective thermal conductivity of the porous medium.

REFERENCES

[1] B. V. Antohe and J. L. Lage, "A general two-equation macroscopic turbulence model for incompressible flow in porous media," *Int. J. Heat Mass Transfer*, vol. 40, pp. 3013-3024, 1997.

[2] D. Getachew, W. J. Minkowycz and J. L. Lage, "A modified form of the model for turbulent flows of an incompressible fluid in porous media," *Int. J. Heat Mass Transfer*, vol. 43, pp. 2909-2915, 2000.

[3] A. Nakayama and F. Kuwahara, "A macroscopic turbulence model for flow in porous medium," *ASME J. Fluids Eng.*, vol. 121, pp. 427-433, 1999.

[4] R. A. Silva and M. J. S. de Lemos, "Turbulent flow in a channel occupied by a porous layer considering the stress jump at the interface," *Int. J. of Heat and Mass Transfer*, vol. 46, pp. 5113-5121, 2003.

[5] Y. Demirel and R. Kahraman, "Entropy Generation in Rectangular Packed Duct with Wall Heat Flux," *Int. J. of Heat and Mass Transfer*, vol. 42, pp. 2337-2344, 1999.

[6] T. V. Morosuk. "Entropy Generation in Conduits Filled with Porous Medium Totally and Partially," *Int. J. of Heat and Mass Transfer*, vol. 48, pp. 2548-2560, 2005.

[7] N. Allouache and S. Chikh. "Second Law Analysis in a Partly Porous Double Pipe Heat Exchanger," *ASME, Journal of Applied Mechanics*, vol. 73, pp. 60-65, 2006.

[8] N. Allouache and S. Chikh. "Numerical modeling of turbulent flow in an annular heat exchanger partly filled with a porous substrate,"*Journal of Porous Media*, vol. 7, pp. 617-632, 2008.

[9] F. Kock and H. Herwig. "Entropy Production Calculation for Turbulent Shear Flows and their Implementation in CFD Codes," *Int. J. of Heat and Fluid Flow*, vol. 26, pp. 672-680, 2005.